Proceedings of ASME Turbo Expo 2011
GT2011
June 6-10, 2011, Vancouver, British Columbia, Canada

GT2011-45502

A METHOD TO ESTIMATE THE PERFORMANCE MAP OF A CENTRIFUGAL COMPRESSOR STAGE

Michael Casey[1] and Chris Robinson

PCA Engineers Limited, Studio 2, Deepdale Enterprise Park, Deepdale Lane,
Nettleham, Lincoln LN2 2LL, UK

[1]Also Institute of Thermal Turbomachinery, University of Stuttgart, Pfaffenwaldring 6,
D-70569 Stuttgart, Germany

ABSTRACT

A novel approach to calculate the performance map of a centrifugal compressor stage is presented. At the design point four non-dimensional parameters (the flow coefficient ϕ, the work coefficient λ, the tip-speed Mach number M and the efficiency η) characterize the performance. In the new method the performance of the whole map is also based on these four parameters through physically-based algebraic equations which require little prior knowledge of the detailed geometry. The variable empirical coefficients in the parameterized equations can be calibrated to match the performance maps of a wide range of stage types, including turbocharger and process compressor impellers with vaned and vaneless diffusers. The examples provided show that the efficiency and the pressure ratio performance maps of turbochargers with vaneless diffusers can be predicted to within ± 2% in this way. More uncertainty is present in the prediction of the surge line, as this is very variable from stage to stage. During the preliminary design the method provides a useful reference performance map based on earlier experience for comparison with objectives at different speeds and flows.

NOMENCLATURE

a_1 = inlet speed of sound (m/s)
a,b,A,B,C,D,E,F,G, and H = coefficients in equations
b_2 = impeller outlet width (m)
c = absolute velocity (m/s)
c_s = slip velocity (m/s)
D_2 = impeller tip diameter (m)
h = specific enthalpy (J/kg)
$k_{\lambda d}$ = coefficient in equation 13 (-)
k_{df} = disc friction coefficient (-)
M = tip speed Mach number (-)
n = polytropic exponent
p = static pressure (N/m^2)
P, t = coefficients in logistic function (-)
u_2 = impeller blade tip speed (m/s)
$\dot{V}$ = volume flow rate (m^3/s)

Greek Symbols

β_2 = impeller blade back-sweep angle (°)
γ = isentropic exponent (-)
γ_d = degree of reaction (-)
η = polytropic efficiency (-)
λ = work input coefficient (-), $\lambda = \Delta h / u_2^2$
ψ = pressure rise coefficient (-)
ϕ = global flow coefficient (-), $\phi = \dot{V} / u_2 D_2^2$
ϕ_2 = impeller outlet flow coefficient (-)
ω = angular velocity (radians/s)

Subscripts

0 = at $M = 0$
1 = inlet total conditions
2 = outlet total conditions
c = choke point
d = design point
Euler = Based on Euler equation
HI = at high speed
i = value on the ith speed line
LO = at low speed
m = meridional component
p = peak efficiency point
s = isentropic, stall
t = total
u = circumferential component

INTRODUCTION

An important requirement during the preliminary design of a centrifugal compressor stage is the calculation of a reliable performance map as a guide to the expected operating flow range and the sensitivity to speed variations when the design is completed. With this information the designer can assess if the design will be suitable for the application. For example, it is possible to check if a new design will provide adequate efficiency, pressure ratio and surge margin on the low speed characteristics and sufficient choke margin at high speeds.

This paper presents a new engineering approach to estimate the performance map for such preliminary design applications. This is a difficult task as the final detailed geometry (such as throat areas, blade angles, blade number, blade thicknesses, etc.) and many aspects of the aerodynamic design (diffusion levels, flow angles, etc.) have not been finalized at this point. An additional difficulty is that the performance map is needed very quickly, typically during engineering discussions on a proposed new development. The most accurate methods of determining the map for competing design solutions, by first completing the design and then making CFD simulations or even measurements, are not suitable in this time-frame.

In some cases, the new stage may be sufficiently similar to a stage that has previously been tested such that the map of this stage can be quickly scaled to give a good estimate of the expected performance. The scaling approach is limited in that it only works if such data is available, and will not work well if the design point of the new stage is sufficiently different from previous experience, especially if the back-sweep and work coefficient have changed as this changes the slope of the flow versus work characteristic. In addition the scaling of maps provides no parametric description, gives no speed-lines at higher or lower speeds than those tested and does not provide a useful reference based on the best experience derived from many different stages.

The common alternative to these approaches is to use empirical correlation based methods for predicting performance maps. Such methods require fairly detailed information of the stage geometry, at least on a one-dimensional (1D) basis. Examples of 1D methods are given by Swain (2005), Aungier (2000), Oh et al. (1997) and Cumpsty (1989). The authors' experience with such methods, however, is that they often require fairly tedious tweaking of coefficients in the empirical models to generate a satisfactory performance map, and that the characteristic curves often have unreliable shapes.

The approach proposed here is based on the fact that well-designed state-of-the-art compressor stages for a particular aerodynamic duty tend to have fundamentally similar shapes of their efficiency performance maps. This indicates that the duty itself is an excellent guide to the form of the performance map. The method proposed is entirely novel in that it uses four key non-dimensional parameters at the design point to determine the performance map, rather than the geometry of the stage.

The method has been applied to a wide range of stage types, which are categorized here as turbocharger or process style impellers, with vaned and vaneless diffusers, giving four categories. Turbocharger impellers (which are similar to gas turbine impellers) are relatively long and un-shrouded, have an axial inlet designed with an inducer and are equipped with thin blades and splitter vanes to make them suitable for transonic flow. Process style impellers in multistage compressors are shrouded and shorter, they usually have radial inlets, have thick blades most often with no splitter vanes and are generally designed for lower Mach numbers. The emphasis of the paper is on the application of the method to predict performance maps for turbocharger style impellers with vaneless diffusers, but examples are also given of some other categories of stage to demonstrate the validity of the method over many applications.

The paper is organized as follows. First, some background to the key non-dimensional parameters and their significance in this method is given. This is followed by a description of the algebraic equations used to parameterize the efficiency performance maps, which explains how these equations allow the physical features of the maps to be modeled for variations of flow and speed. The calibration of the coefficients in the efficiency equations using test data from several sources is then provided. A subsequent section describes the equations used for the variation of the work coefficient with flow and speed, and the validation of these. A difficult aspect is the prediction of surge and the pragmatic solution to this is described in the penultimate section. Finally the paper demonstrates the use of the equations to predict typical turbocharger performance maps. A discussion of the results leads to the conclusions.

BACKGROUND TO THE METHOD

The objective is to calculate the values of two dependent variables (the polytropic efficiency and work coefficient) for specific values of the independent variables (the flow coefficient and tip-speed Mach number):

$$\eta, \lambda = f(\phi, M) \qquad (1)$$

All other thermodynamic performance information can then be calculated from these variables, such as isentropic efficiency, pressure ratio, volume flow, and mass flow. Speed lines can then be generated for specific values of the tip-speed Mach number by varying the flow coefficient and the full map comprises an array of speed-lines with different tip-speed Mach numbers. The equations describing the functional dependency of these variables include several non-dimensional parameters, many variable coefficients and some fixed constants, and are described in the sections below.

Before we consider these equations, it is worthwhile to consider the four key non-dimensional parameters that are used:

- The expected design point polytropic efficiency, η
- The global volume flow coefficient, ϕ
- The stage work coefficient, λ
- The stage tip-speed Mach number, M

These values are the typical results of a preliminary design process based on 1D performance correlations. Together with the inlet flow conditions, gas properties and impeller diameter, they define the design point duty by the following equations:

$$\phi = \dot{V} / u_2 D_2^2, \quad \lambda = \Delta h / u_2^2, \quad M = u_2 / a_1$$

$$\frac{p_2}{p_1} = \left[1 + (\gamma - 1)\lambda M^2\right]^{\frac{\eta\gamma}{\gamma-1}} \tag{2}$$

$$\dot{V} = \phi u_2 D_2^2 = \phi M a_1 D_2^2$$

At first sight it may be surprising that these non-dimensional parameters also define the shape of the performance map with no detailed information about the stage geometry. However, the design values of flow coefficient, work coefficient, efficiency and tip-speed Mach number determine the details of the stage geometry in the subsequent design. If this design is done well then the performance characteristic for this optimally designed stage can be implied from these design values.

Consider a stage designed for a certain flow coefficient and tip-speed Mach number with an optimally matched vaned diffuser. If the diffuser vane setting angle were changed to give a lower throat area, then the matching between the impeller and diffuser would change and the value of the flow coefficient at peak efficiency would be reduced. Thus a change in the value of the design flow coefficient would characterize this change in geometry. Alternatively the smaller diffuser could be considered to be a diffuser that is better matched at a higher tip-speed for the same flow coefficient, so the effective design Mach number of the stage would be increased by this geometrical change. In this way the values of the flow coefficient and tip-speed Mach number at the design point include information about the optimal geometry and internal stage matching and can be used to characterize this. Exactly which geometrical features are needed to meet the performance target is the objective of the preliminary design and detailed design but a good estimate of the map is possible without this information.

The design point efficiency, η, is defined as the polytropic efficiency; this defines the aerodynamic quality of the design and allows a simple extension to multistage machines without so-called reheat factors to account for the divergence of the isobars in a T-s diagram. It is assumed that some system of correlations, is available to characterize all the losses at the design point, and this aspect of the preliminary performance prediction technique is not described in any more detail here.

The non-dimensional inlet flow coefficient, ϕ, characterizes the stage type, the flow channel width and also provides a guide to the efficiency level that may be expected, see Cumpsty (1989). Well-designed radial compressors have a value of the flow coefficient close to $\phi = 0.09 \pm 0.01$.

The stage work coefficient, λ, characterizes the work input of the stage, including parasitic disc friction losses. Typical values are $\lambda = 0.65 \pm 0.1$. This parameter is determined essentially by the outlet velocity triangle of the impeller, and so characterizes the effect of blade number, impeller outlet width and back-sweep angle on the work input.

The stage tip speed Mach number, M, characterizes the local Mach number levels in the stage and loading in terms of the stage pressure and temperature ratio. Typical industrial process compressor stages have tip speed Mach numbers between 0.5 and 1.0, turbochargers for automotive applications between 0.5 and 1.5, turbochargers for larger diesel engines between 0.8 and 1.7, and gas turbine compressors and refrigeration compressors from 1.0 to 2.0. At the design condition the density variation through the stage defines the local meridional velocity levels, velocity triangles and the work input of the stage. Operation at other speeds will cause a change in the density variation and the change in velocity triangles leads to a different matching of the components, probably with a lower performance, and a shift in volume flow coefficient. The method described here captures these effects of a change of speed away from the design point, at least on a global basis.

For map prediction additional information is also needed to characterize the variation in performance away from the design point, which will differ for different stage types. For example, stages with a vaneless diffuser tend to have a wider operating range than stages with a vaned diffuser. Equations are needed for the variation in the best point efficiency and flow on different speed-lines and for the variation in performance with flow along each speed-line. In addition the change in work with flow and tip-speed needs to be captured. The equations described below provide a parameterized description of the performance map, whereby different values of the empirical coefficients are used to model the characteristics for different types of compressor stage but the structure of the equation system remains the same for all compressors.

VARIATION OF EFFICIENCY WITH FLOW AND SPEED

Equations for the variation of efficiency with flow

The equations used to describe the variation of efficiency with the flow go back to the system described in diagrams by Rodgers (1964). Rodgers showed various diagrams, similar to figure 1, in which the variation of normalized efficiency with normalized flow is modeled with an equation of the form

$$\frac{\eta}{\eta_p} = f\left(\frac{\phi}{\phi_c}, M\right) \tag{3}$$

where the ratio of the efficiency relative to that at the peak efficiency point (η/η_p) is a function of the flow coefficient relative to the maximum flow coefficient at choke (ϕ/ϕ_c) and the tip-speed Mach number. The lines plotted in figure 1 are an example of those described by the equations given below and are not taken from Rodgers. The key aspect is that at low tip-speed Mach numbers the operating range is largest and the flow at peak efficiency is then furthest from the choke conditions.

The same information is presented in figure 2, but plotted relative to the flow at peak efficiency (ϕ/ϕ_p). The form shown in figure 2 is needed in this method, as in the preliminary design phase the design flow is known and the choke flow is not known as the throat areas have still to be determined.

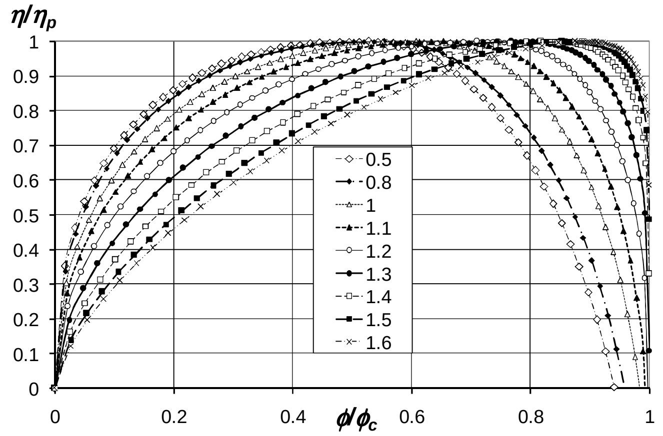

Figure 1: Variation of efficiency ratio with the ratio of the flow coefficient relative to that at choke for a range of tip-speed Mach numbers.

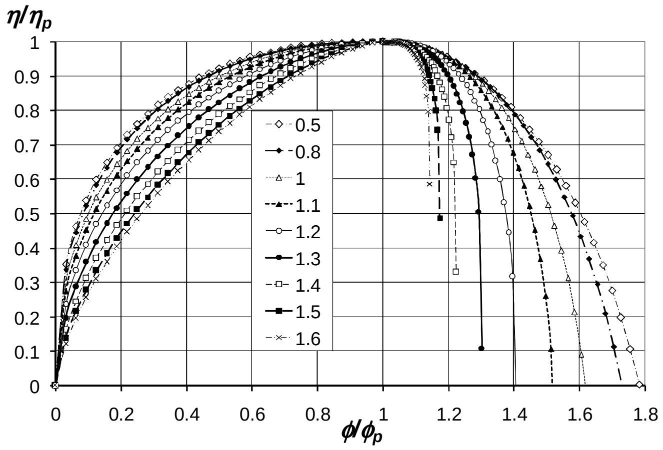

Figure 2: Variation of efficiency ratio with the ratio of the flow coefficient relative to that at peak efficiency for a range of tip-speed Mach numbers.

Rodgers (1964) gave no equations for these curves but in several publications (Swain (1990), Casey (1994) and Swain (2005)) some analytic equations for such curves have been described. After extensive experimentation with these published equations, and many other forms, a new more physically based equation structure has been developed. Clearly the equations used are not actually a real physical model of the losses but a particular structure has been chosen in order to reproduce important physical effects in the stage characteristics.

In the current work the variation of stage efficiency with flow along a speed line is a modified form of an elliptic curve:

$$\frac{x^2}{a^2}+\frac{y^2}{b^2}=1, \quad \frac{x}{a}=\left[1-\left(\frac{y}{b}\right)^2\right]^{1/2} \tag{4}$$

For flows below the peak efficiency point this equation is modified to have a variable exponent to give the characteristic curves for efficiency ratio as a function of flow ratio as follows

$$\phi<\phi_p, \quad \frac{\eta}{\eta_p}=\left[1-\left(1-\frac{\phi/\phi_c}{\phi_p/\phi_c}\right)^D\right]^{1/D} \tag{5}$$

This equation has the natural physical property that the efficiency is zero at zero flow coefficient and the curves have a maximum at the flow coefficient for peak efficiency (ϕ_p/ϕ_c), and are horizontal at this point. To match the test data the coefficient *D* takes different values for different tip-speed Mach numbers and this provides a small Mach number dependency on the shape of the characteristics in the low flow region, see figure 2. For turbocharger stages with vaneless diffusers the typical value of *D* varies from 2.1 on the low speed characteristics to 1.7 on the high speed characteristics, and this is clearly related to the physical increase in the strength of the incidence losses at high Mach numbers. The equations do not include any specific details related to flow separation or instability at low flows and retain a simple ellipse-like shape down to zero flow. This is a weakness in the prediction of the onset of instability as in reality relatively small changes in the slope of the pressure rise variation with flow can cause the onset of instability.

For flows above the peak efficiency these equations are further modified to take account of the fact that when the maximum flow is reached, the efficiency may differ from zero:

$$\phi>\phi_p, \quad \frac{\eta}{\eta_p}=(1-G)+G\left[1-\left(\frac{\dfrac{\phi}{\phi_c}-\dfrac{\phi_p}{\phi_c}}{1-\dfrac{\phi_p}{\phi_c}}\right)^H\right]^{1/H} \tag{6}$$

This equation has a similar ellipse-like shape to the equations below the peak efficiency point and this leads to a smooth transition between the two arcs around the peak efficiency. The curves automatically have the maximum efficiency at the flow coefficient for peak efficiency and have the maximum flow with a vertical characteristic at the flow coefficient for choke. The coefficients *H*, *G* and the ratio of the flow coefficient at peak efficiency to that at choke, (ϕ_p/ϕ_c), are not constant but also vary with the tip speed Mach number to give narrower characteristics of different shape as the Mach number increases, see figure 2.

The exponent *H* has a similar function to the exponent *D* in equation 5. This exponent takes into account the fundamentally different shapes of efficiency characteristics for low Mach number and high Mach number impellers. Low Mach number impellers tend to have a smooth drop in efficiency ratio related to incidence losses as the flow increases above peak efficiency. A value of *H* near to 2, giving elliptical curves, is needed to match low-speed experimental data. High Mach number stages tend to have a small plateau of high efficiency close to the peak efficiency point and then drop much more sharply into choke. To match experimental data on the shape of high Mach number characteristics a value of $H=3.5$ is needed, which is close to the exponent of 4 used by Swain (2005).

Equation 6 includes an additional change to account for the fact that the location of maximum flow at choke is not necessarily at zero efficiency, but at an efficiency ratio of (*1-G*). High Mach number impellers reach choke at relatively high efficiency (with $0>G>1$), or even at peak efficiency if all sections operate at unique incidence conditions, see Lohmberg et al. (2003). The vertical choked characteristics start immediately below this point and not when zero efficiency has been reached, as shown in the high Mach number curves in figure 2. In contrast, low Mach number impellers fall to an efficiency of zero well before the maximum choke flow is reached (with $G>1$), as high losses due to negative incidence stall occur before choke, see Casey and Schlegel (2010). The flow continues to increase below the point of zero efficiency, as also shown in the low Mach number curves of figure 2. In this way *G* is also a function of the tip-speed Mach number.

The analysis of test data for typical turbocharger style stages indicates that at high speeds a value of $G = 0.3$ is needed – indicating that choke occurs at an efficiency ratio of 0.7. At low speeds a value of $G = 2$ is needed, which indicates that choke occurs well down the characteristic when the efficiency ratio reaches -1. The diagrams shown by Casey (1994) include this effect but are simply elliptical at all speeds with $H = 2$. The equations of Swain (2005) do not include these choking effects and always become vertical at a maximum flow at zero efficiency ratio, as they effectively have a value of $G = 1$. Neither system includes any variability of the strength of incidence effects below the peak efficiency point.

Variation of coefficients with Mach number

Equations 5 and 6 include many variable coefficients which depend only on the tip-speed Mach number. These coefficients are constant along each speed-line but vary from one speed-line to the next. At low-tip speed Mach numbers the flow is effectively incompressible and there is only a small effect of Mach number, so the coefficients have a constant value at low speeds. Analysis of test data, see below, has identified that the coefficients also tend to have a constant value at high tip-speed Mach numbers, indicating that the normalized shape of the high speed characteristics no longer changes with Mach number. In the current method the coefficients for intermediate Mach numbers are then determined from the two asymptotic values at low speed and at high speed with the use of a blending function.

This procedure is demonstrated with regard to the ratio of the flow coefficient at peak efficiency to the flow coefficient at choke (ϕ_p/ϕ_c), which appears in equation 6. A low value of this coefficient indicates a high operating range between peak efficiency and choke. Experience shows that the operating range of compressors is largest at very low Mach numbers and remains constant at low Mach numbers. The range then decreases with increasing Mach number but again remains more or less constant at much higher Mach numbers. Equations have been selected which include this feature as a natural property:

$$\frac{\phi_p}{\phi_c} = (1-P)\left(\frac{\phi_p}{\phi_c}\right)_{LO} + P\left(\frac{\phi_p}{\phi_c}\right)_{HI}$$
$$P = \frac{1}{1+e^{-t}}, \quad t = (M-B)(AM+C) \tag{7}$$

The parameter *P* in this equation is the s-shaped logistic function, and varies from 0 to 1 with increasing tip-speed Mach number. It blends the values of the coefficients between the low tip-speed Mach number asymptote (subscript *LO*) and the high tip-speed Mach number asymptote (subscript *HI*). At low Mach number the variation with Mach number is small as *P* remains close to 0, which is physically realistic as the flow is effectively incompressible up to $M = 0.3$. At high Mach number the equations also attain a constant asymptotic value with P close to 1, which matches experience that the form of the characteristics remains similar at high Mach numbers. The transition between these extreme values reaches the halfway value between the upper and lower asymptotic values with a value of $P = 0.5$ with $t = 0$ at a Mach number of $M = B$, and the rate of transition around this value is determined by the constants *A* and C.

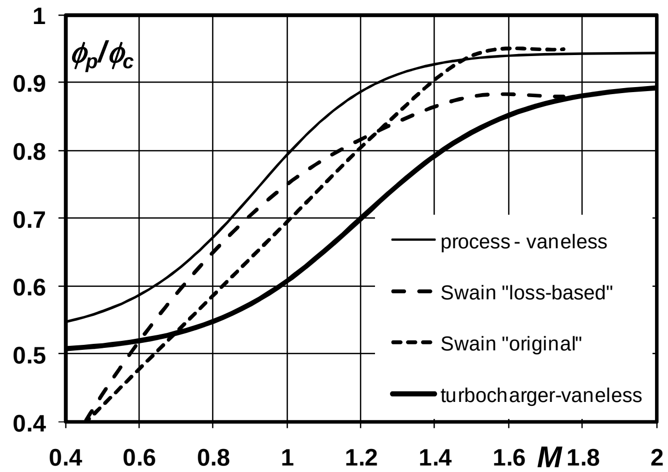

Figure 3: Ratio of the flow coefficient at peak efficiency to that at choke over a range of tip-speed Mach number.

Different types of stages (process or turbocharger impeller, vaned and vaneless diffuser) have different coefficients for the ratio of ϕ_p/ϕ_c at high and low Mach numbers. Vaneless diffuser stages tend to have lower values of this ratio than vaned diffuser stages as vaned diffusers are usually matched such that they choke before the impeller and this limits the range of the stage giving a larger value of ϕ_p/ϕ_c. Two lines demonstrating the value ϕ_p/ϕ_c for different coefficients are shown in figure 3. The upper thin curve models process stages with vaneless diffusers (with impellers having thick blades and no splitters) and the lower thick curve models modern turbocharger stages with vaneless diffusers. Other curves are needed for vaned diffusers. Swain has suggested 2 forms of variation of this ratio with the Mach number, but supplied no equations for this. These are shown as dashed lines in figure 3 – the shorter dashes are Swain's original correlation and the longer dashes are his recent "loss-based" curve, see Swain (2005). Note that the curves of Swain show broadly similar trends, although they are derived for the impeller only, except at very low Mach numbers where the trend of Swain appears unrealistic as at low Mach numbers constant values are expected. It should be noted that at low speeds it is in any case difficult to be precise about choking as no test data ever reaches this condition.

The coefficient *B* in equation 7 can be envisaged as a measure of the transonic capability of the stage, or as a sort of critical tip-speed Mach number of the design. Analysis of test data has shown that typical turbocharger stages tend to require a value of B of around 1.1 or 1.2 to match their characteristics. Process style stages in multistage compressors tend to require a value of *B* of around 0.8 to 0.9. In all stages examined a good match with the transition over the range of Mach numbers was given with values of *A* between *0* and *1* and *C* between *4* and *5*.

The coefficients *D*, *G* and *H* in equations 5 and 6 make use of a similar approach to determine their values at intermediate Mach numbers from the values at high and low tip-speeds:

$$\begin{aligned} D &= (1-P)D_{LO} + PD_{HI} \\ G &= (1-P)G_{LO} + PG_{HI} \\ H &= (1-P)H_{LO} + PH_{HI} \end{aligned} \qquad (8)$$

The blending function *P* is the same as in equation 7.

The equations given above describe the variation of efficiency with flow relative to that at the peak efficiency point along each speed characteristic. In addition to these equations some additional efficiency equations are needed for the peak efficiency and the flow coefficient at peak efficiency on each speed line. These equations are determined from test data on a more ad hoc basis, as outlined below.

Validation of the efficiency equations with test data

Having defined these equations it remains to demonstrate that these adequately describe the variation of efficiency with flow and speed in real compressor stages. An analysis of more than 45 different compressor stages covering a wide range of applications has been carried out to determine the most suitable values of the coefficients in the equations. The test data covers a variety of state-of-the-art turbocharger and process compressor characteristics from measurements made by a variety of confidential sources and neither the sources nor the original data may be disclosed. Of the many performance maps available to the authors only those for the best stages have been used for the correlations. No further information can be provided, but in all cases attention has been given to the consistency of the data and it is considered to be very sound and reliable with typical efficiency errors in the range ±2%.

With fine tuning of the available coefficients in the equations given above it is possible to match almost exactly the variation of efficiency ratio with flow along any speed line for any specific case, but for the purposes of a general method a fixed set of coefficient values is needed for particular stage types. The typical good agreement using these fixed set of coefficients is shown in figure 4 giving variations of efficiency ratio with flow ratio for a typical turbocharger stage with a vaneless diffuser. The measurement data has been obtained along a number of constant speed lines and the curves are the calculated variations at these speeds using the equations of this paper. Taking into account inevitable experimental error (probably at least ± 2% on the characteristics of typical turbocharger rigs) the agreement is exceptionally good.

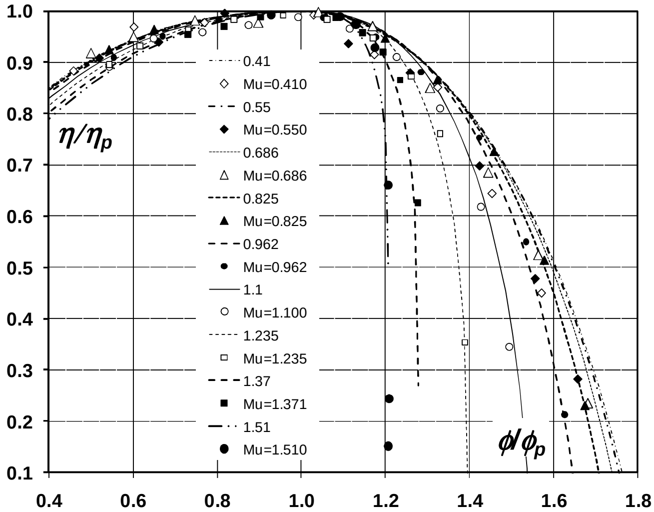

Figure 4 : Normalized efficiency ratio of a vaneless turbocharger stage using equations 5, 6, 7 and 8 compared with test data at different tip-speed Mach numbers

The test data on this case show clearly that there is a need for different characteristic shapes for the efficiency below the peak efficiency point as the Mach number varies, using different values of *D* in equation 5. Note that the coefficients used here have not been selected to match the performance of this particular stage but are the mean values needed to match the performance of a range of similar turbocharger stages. This demonstrates that the method appears to be useful to adapt knowledge gained on the operating range of one stage to provide a reference for another of a similar type.

The equations for the variation of the ratio of the flow coefficient at peak efficiency to the maximum flow coefficient at choke (ϕ_p/ϕ_c) have also been determined from test data. The values at very low Mach number have been calibrated from data published by Gülich (2005) for the operating range of centrifugal pumps (with $M = 0$), and this causes the trend at low Mach numbers to differ from the curves of Swain, as already indicated in figure 3. At higher Mach numbers the validation process is slightly more difficult and requires some fine engineering judgment. Firstly, the test data towards choke usually do not have sufficiently low pressure ratios that the maximum flow at choke is achieved, especially on the low Mach number speed-lines. Secondly, the efficiency curves are very flat near the peak efficiency point and the small number of test points along each characteristic combined with the experimental error does not uniquely define the flow coefficient at the peak efficiency point. These issues have been tackled by using the equations given here to model each characteristic individually and to determine the required flow ratio (ϕ_p/ϕ_c) from the modeled characteristics. Figure 5 shows the variation of the flow ratio determined by this process from the analysis of test data from several turbocharger stages with a vaneless diffuser. In these cases with turbocharger style impellers the choke flow is defined by the choke of the impeller inlet. The differences are related to the different throat areas, blade thicknesses and shroud diameter of the different impellers.

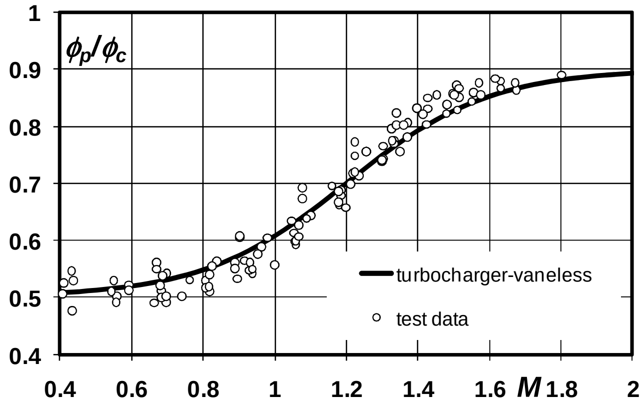

Figure 5: Ratio of the flow coefficient at peak efficiency to that at choke over a range of tip-speed Mach number for turbocharger compressor stages with a vaneless diffuser.

Figure 6 shows the additional characterization of the variation of the flow coefficient at peak efficiency with Mach number for stages with vaneless diffusers. The bottom axis is the impeller tip speed Mach number and the vertical axis shows the variation of flow coefficient at peak efficiency relative to that at a low tip-speed Mach number. The process compressor stages are shown as solid symbols and are modeled empirically by the full curve shown. The open symbols represent turbocharger style stages and are modeled by the dashed line.

The flow coefficient at the peak efficiency point tends to increase as the tip speed Mach number increases. This is caused partly by the effect of the change in the density on the velocity triangles at impeller inducer inlet with speed. It is also related to the mismatch with the diffuser as this becomes too small for the impeller at low speeds forcing the peak efficiency of the stage to move to a lower flow coefficient. At very high tip-speed Mach numbers there is a drop in the flow coefficient at peak efficiency related to the onset of choking in the impeller inlet, which clearly happens earlier in process stages. This is believed to be related to the general use of thicker blades and a lack of splitter vanes in process compressors. Polynomial equations have been developed for the curves shown here.

Figure 7 shows the variation of the peak efficiency, relative to that at the design point over a range of tip speed Mach numbers. The horizontal axis is the ratio of the Mach number to the design Mach number. Here the scatter appears to be very large but this is slightly deceptive. The test data includes many of turbocharger stages whose apparent efficiency drops rapidly towards low tip-speed Mach number, as depicted by the dotted line. This is not an aerodynamic effect but is an error in efficiency measurement due to ignoring the heat transfer effects from the turbine in the efficiency determination on a turbocharger test rig; see Casey and Fesich (2010). The strength of this effect depends on the amount of heat transfer, and for adiabatic stages there is only a small fall in efficiency as the Mach number is reduced below the design point. The experimental error in the efficiency determination in these tests is probably not better than ± 2%.

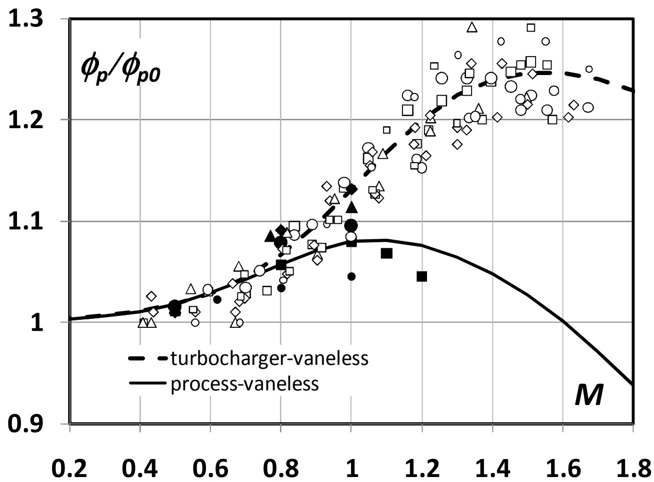

Figure 6: Ratio of the flow coefficient at peak efficiency to that at low speed over a range of tip-speed Mach number for vaneless stages. Turbocharger compressor stages shown as a dashed line and open symbols and process compressor stages shown as a full line and full symbols.

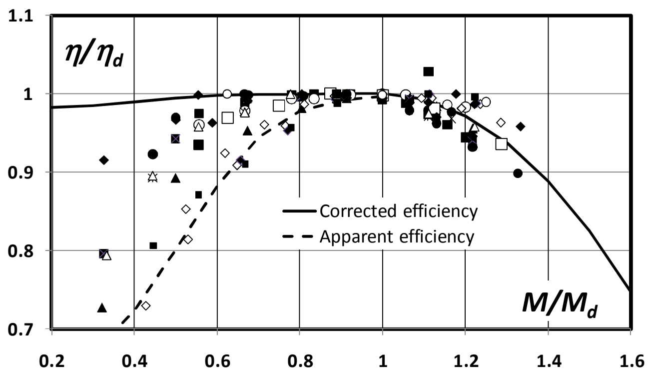

Figure 7: Ratio of peak efficiency to that at design over a range of tip-speed Mach number for stages with vaneless diffusers, with and without the correction for heat transfer effect

Summary of the calculation procedure for the efficiency

For the calculation of efficiency on a given speed line, the first step is to calculate the values of the variable coefficients (D, G, H and ϕ_p/ϕ_c) that correspond to this tip-speed Mach number, from equations 7 and 8. The peak efficiency and the flow coefficient at peak efficiency need to be determined from the equations for the curves shown in figures 6 and 7. For a given inlet flow coefficient this then allows the efficiency to be determined from equations 5 for flows below the peak efficiency or equation 6 for higher flows.

At this point it is useful to summarize what has been achieved with regard to the prediction of efficiency. The objective was to calculate the value of the polytropic efficiency for specific values of the independent variables (the flow coefficient and tip-speed Mach number). A completely new set of parametric equations has been developed for this purpose, based on the key non-dimensional parameters which determine the performance at the design point. The equations describing this functional dependency are physically realistic. They also include many variable coefficients (which are a function of the tip-speed Mach number) and some fixed constants, and typical values of these have been given above. The excellent agreement shown in figure 4, which is typical of other cases, demonstrates that the objective has been achieved with these equations and coefficients for turbocharger style stages to within an error band of roughly ± 2% in the efficiency, which probably corresponds to the accuracy of these measurements.

VARIATION OF WORK INPUT COEFFICIENT

The second part of the functional relationship of equation 1 is the variation of the work input coefficient with flow and tip-speed Mach number. This variation is based on the Euler equation following an approach described by Casey and Schlegel (2010). Under the assumption that the flow has no swirl at inlet to the impeller, then the Euler work due to the adiabatic work input of the impeller can be approximately estimated from the velocity triangles. The work is related directly with the flow coefficient at impeller outlet $\phi_2 = c_{m2}/u_2$, the assumed slip velocity c_s/u_2 and the impeller outlet blade angle β_2', as follows:

$$\lambda_{Euler} = \frac{c_{u2}}{u_2} = 1 - \frac{c_s}{u_2} + \phi_2 \tan\beta_2' \qquad (9)$$

Note that the impeller outlet angle is negative for a backswept impeller with the notation used here. For a constant value of the slip factor the work input coefficient can be expected to decrease linearly with the impeller outlet flow coefficient.

We convert equation 9 into a form which takes the density change from the stage inlet to the impeller outlet into account; so that the flow coefficient based on the inlet volume flow can be used, as follows:

$$\phi_2 = \phi \frac{1}{\pi} \frac{D_2}{b_2} \frac{\rho_{t1}}{\rho_2} \qquad (10)$$

If we consider compression in the impeller as a polytropic process with a kinematic degree of reaction of γ_d, see Casey and Schlegel (2010), and a polytropic exponent of n_d, then the density ratio from inlet to outlet can be derived as

$$\frac{\rho_2}{\rho_{t1}} = \left[1 + (\gamma - 1)\gamma_d \lambda M^2\right]^{\frac{1}{n_d - 1}} \qquad (11)$$

and the Euler work input coefficient can be expressed in terms of the inlet volume flow coefficient as

$$\lambda_{Euler} = 1 - \frac{c_s}{u_2} + \frac{\phi D_2}{b_2 \pi} \frac{\tan\beta_2'}{\left[1 + (\gamma - 1)\gamma_d \lambda M^2\right]^{\frac{1}{n_d - 1}}} \qquad (12)$$

When operating at a flow coefficient near to the peak efficiency point, backswept impellers have a fairly constant value of the degree of reaction (around 0.6), so this and the slip factor are taken as constant along the characteristic. The polytropic exponent can be approximated from the stage efficiency.

The design value of the work coefficient includes not only the Euler work but also the disc friction work so that:

$$\lambda_d = \lambda_{Euler\_d} \left(1 + \frac{k_{df}}{\phi}\right) \qquad (13)$$

Where the value of k_{df} is a disc friction coefficient and can typically be taken as 0.003 or calculated from the design value of the disc friction power using correlations from Daly and Nece (1960). The Euler work coefficient varies linearly with flow so that from equation 12 at the design point we derive a linear expression at the design tip-speed Mach number and then have

$$\lambda_{Euler\_d} = 1 - \frac{c_s}{u_2} + \phi_d k_{\lambda d} \qquad (14)$$

The value of the coefficient in this equation, which is the slope of the Euler work coefficient curve with a variation in the flow, can be determined at the design point as

$$k_{\lambda d} = \left(\lambda_{Euler\_d} - 1 + \frac{c_s}{u_2}\right) / \phi_d \qquad (15)$$

The slip factor is assumed to stay constant and needs to be specified, but the coefficient for the slope changes with the Mach number, as can be seen in equation 12. An approximate relationship for this slope, which is related to the change in density at impeller outlet with speed follows from equation 12, and assumes that the impeller efficiency is similar to the stage efficiency so that the polytropic exponent can be calculated:

$$\frac{k_{\lambda i}}{k_{\lambda d}} = \frac{\left[1 + (\gamma - 1)\gamma_d \lambda_d M_d^2\right]^{\frac{1}{n_d - 1}}}{\left[1 + (\gamma - 1)\gamma_d \lambda_d M_i^2\right]^{\frac{1}{n_d - 1}}} \qquad (16)$$

Equations 15 and 16 provide the slope of the work coefficient curve at each speed and the complete equation for the variation of the work coefficient with flow and tip speed Mach number is then given as

$$\lambda_i = \left(1 + \frac{k_{df}}{\phi_i}\right)\left(1 - \frac{c_s}{u_2} + \phi_i k_{\lambda i}\right) \tag{17}$$

In this expression index i represents the different speed lines.

The novel aspect of these equations is that the variation of the work coefficient with flow is calculated with no prior knowledge of the impeller outlet velocity triangle or geometry. The value of the work coefficient at the design flow coefficient together with the slip factor determines the slope of the work input characteristic at the design speed. The slope is then adjusted to take into account the effect of the speed on the work input, via the density change at impeller outlet. The determination of this slope in this way eliminates the need for any specific knowledge of the blade geometry and ensures that the flow-work characteristic is in accordance with the Euler equation.

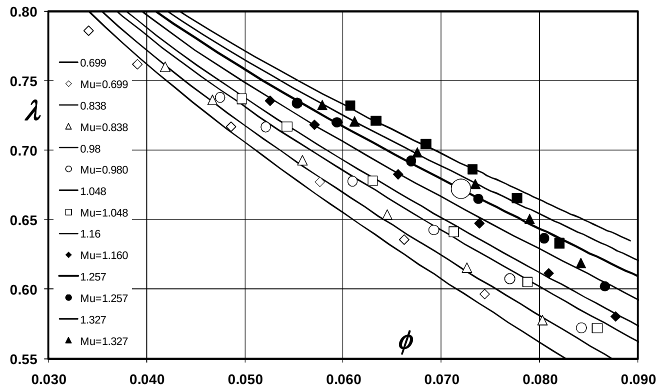

Figure 8: Variation of work coefficient with flow and tip-speed Mach number for a turbocharger stage with a vaneless diffuser.

<u>Validation of work coefficient curves with test data</u>

The available test data has been used to examine the variation of work coefficient with flow and Mach number. Note that it is necessary to define a value of the slip factor (typically in the range 0.1 to 0.2), a value of the disc friction coefficient (typically between 0.002 and 0.004) and the degree of reaction (typically between 0.50 and 0.65) for these curves, so that some limited additional information about the stage geometry is useful for this. As this information is usually known early in a preliminary design process this is not difficult.

Figure 8 shows an example of a turbocharger impeller tested with a vaneless diffuser in a dedicated compressor test stand, which avoids the heat transfer effects on the work coefficient found in turbocharger gas stands. The large white dot in the middle of the diagram is the design point of the stage at a tip-speed Mach number of 1.25 and the variation of the work coefficient with flow and with Mach number on different characteristics (from 0.6 to 1.45) away from this point is well captured by the equations above. The symbols are the measured work coefficient values roughly situated on the lines determined from the equations. Note that the equations reproduce the increase in work coefficient as the flow reduces and the change in work with tip-speed Mach number. This determines the slope of the pressure rise characteristic, which is different for different stages, and would not be obtained by a simple scaling of measured characteristics. The method, as described here, does not capture the additional fall in work coefficient as the impeller chokes towards high flow on the high speed characteristics, but a method to include this has already been described by Casey and Schlegel (2010), and is currently being included in the method.

PREDICTION OF STABILITY LIMIT

One of the most difficult aspects of compressor flows is the prediction of the stability limit due to the onset of rotating stall or surge. The difficulty is exacerbated by the fact that different components (diffuser or impeller) may be responsible for the instabilities, different phenomena may occur (rotating stall, and surge), test procedures to identify instabilities may differ and that the compression system itself may play a role.

With such a large number of effects it is not surprising that any systematic comparison of different stages shows the wide variability of the operating range of compressor stages. As an example of the typical large amount of scatter, Baines (2005) shows that the ratio of the flow at the onset of instability relative to that at choke may vary by at least a factor of 2 for a range of different designs. It is clearly not possible in a preliminary design method with no detailed information on the internal aerodynamics, geometry and loading of the stage to predict the stability point exactly. In fact, even with more detailed knowledge of the geometry and internal flow, and even with the help of computational fluid dynamics, it is still exceptionally difficult to predict the onset of instability with any certainty.

The best that can be done in the framework of this method is to derive a logically consistent set of equations for the variation of the flow at the stability point, and to suggest a range of typical coefficients that can be used in these equations to express an optimistic, a realistic and a pessimistic stability line. A summary of the instability points of the vaneless turbocharger stages that have been analyzed is presented in figure 9. This shows the ratio of the measured flow coefficient at the onset of instability relative to that at the choke point (ϕ_s/ϕ_c) on each speed line, as denoted by the tip-speed Mach number. The large scatter is immediately apparent and this would be larger if poor quality stages had been included.

The dark symbols are conventional stages without the use of a re-circulating bleed system for enhancing the map width. The open symbols are stages using some form of re-circulating bleed, which clearly improves the operating range on the high speed characteristics. This diagram also includes the upper and lower limits of the correlation of Baines (2005) as dotted lines. Note that the original curves of Baines are expressed in terms of a pressure ratio and here these have been converted approximately to a tip-speed Mach number using sensible engineering assumptions.

The lowest operating range of the well-designed stages examined is slightly better than the correlation of Baines and the dot-dashed line shows the equations developed for this pessimistic variation of the instability point. The other dashed line expresses the correlation for stages with a wide range and this agrees partly with the upper optimistic limit quoted by Baines. The full line in this diagram is the pragmatic equation used for a mean range, which is considered realistic for a well designed stage. This is based on the equations already described for the peak efficiency to choke flow ratio (ϕ_p/ϕ_c) in equation 8, as modified in equation 18:

$$\frac{\phi_s}{\phi_c} = (1-P)\left(\frac{\phi_s}{\phi_c}\right)_{LO} + P\left(\frac{\phi_s}{\phi_c}\right)_{HI}$$
$$P = \frac{1}{1+e^{-t}}, \quad t = (M - B_s)(A_s M + C_s) \tag{18}$$

The coefficients used for the realistic surge line shown in figure 9 are as follows; $(\phi_s/\phi_c)_{LO} = 0.225$, $(\phi_s/\phi_c)_{HI} = 0.835$, $A_s = 0.0$, $B_s = 1.25$, and $C_s = 4.75$.

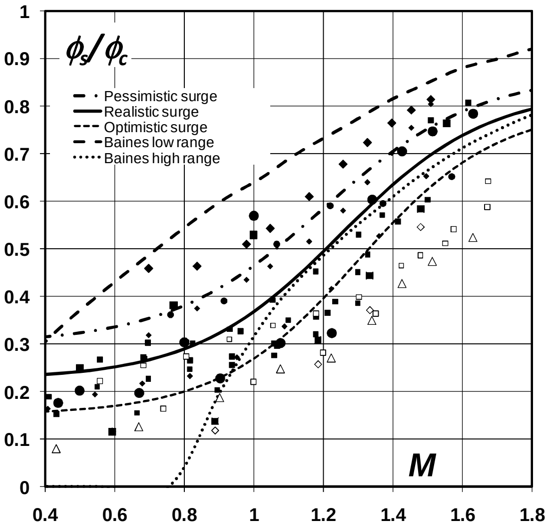

Figure 9: Variation of the ratio of the flow coefficient at instability with that at choke for vaneless turbocharger stages (ϕ_s/ϕ_c). The open symbols are stages with inlet bleed recirculation .

PREDICTION OF OVERALL OPERATING RANGE

During the development of the correlations presented here different ways of comparing the performance of different stage types has been developed. One of these is shown in figures 10 and 11. Figure 10 shows the variation of the choke flow coefficient, the peak efficiency flow coefficient and the surge flow coefficient as a function of the tip-speed Mach number for the typical vaneless diffuser turbocharger stage, and figure 11 shows this variation for a turbocharger stage with a vaned diffuser. In both cases the flow coefficients are normalized relative to the flow coefficient that would occur at peak efficiency at low Mach number, ϕ_{p0}, which is lower than the design flow coefficient. The lines given in these diagrams are the curves given by the equations in this paper, and the points are the measured surge, peak efficiency and choke points of the stages used for validation at different tip speeds.

The variation with tip speed Mach number shown provides a useful presentation of the operating envelope and resembles a typical "alpha-Mach" diagram used to visualize the available operating range of compressor cascades at varying incidence and flow Mach number levels in the preliminary design of axial compressors, see the examples given by Casey (1994). The variation with Mach number of the different lines in these diagrams agrees well with the measurement data and the lines are consistent with each other. This provides further justification for the coefficients used to determine these individual curves

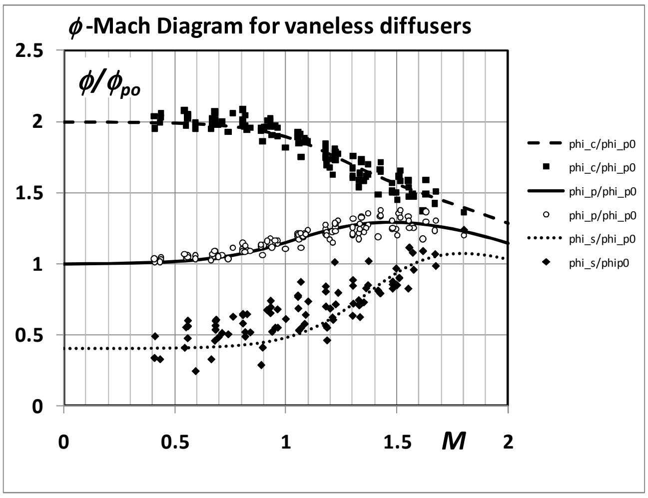

Figure 10: Flow coefficient - Mach number diagram for turbocharger compressors with a vaneless diffuser.

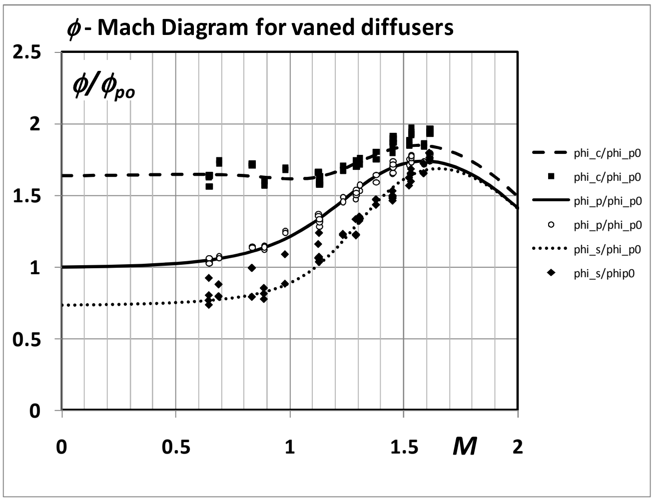

Figure 11: Flow coefficient - Mach number diagram for turbocharger compressors with vaned diffusers.

The difference between these two diagrams also shows up some interesting aspects related to the effect of matching on the characteristics at different speeds. Firstly, the much wider range of stages with vaneless diffusers can be seen from the spacing between the surge and choke lines in these diagrams. Secondly the shift in the flow coefficient at the peak efficiency point with Mach number is very different for the two cases. In the vaned diffuser case, Figure 11, the diffuser is generally matched to the impeller at high speeds and then becomes much too small at low speeds. This causes the impeller to operate at high incidence and forces the stage characteristic to move to a lower flow coefficient. This effect is much less strong in the vaneless diffuser. A vaneless diffuser with no blades can accept higher flows at lower speeds as it does not choke and the impeller is not forced to operate at such a low flow coefficient.

PREDICTION OF PERFORMANCE MAP

As a demonstration of the capability of the method described here, figures 12 and 13 compare the predicted and the measured characteristics of a typical turbocharger compressor stage with a vaneless diffuser over a range of speeds. The measured characteristics were obtained on a turbocharger gas stand using a small compressor impeller with a back-sweep of approximately -30° over a range of speeds from 40,000 to 230,000 rpm. The predictions are based on the equations given in this paper, whereby the coefficients used were derived from a whole range of turbocharger stages. The measured points on all speed lines agree very well (to within ± 2%) with the predictions, and the measured surge line lies typically between the limits of the predicted pessimistic and optimistic lines.

The design point of this stage is denoted as a large open circle on the third fastest speed line. The non-dimensional values of the key parameters (efficiency, flow coefficient, work coefficient and tip-speed Mach number) and the impeller diameter have been specified at this point and all other curves are then calculated from this point using the correlations and equations given in this paper. In addition to these non-dimensional coefficients, the slip factor, the degree of reaction and the disc friction coefficient are specified, whereby standard values from other impellers may be used if these are not known, but no other information on the geometry is needed. As this compressor stage has been tested in a turbocharger with heat transfer from the turbine, the efficiency shown here includes a correction for the effect of heat transfer according to the approach of Casey and Fesich (2010), whereby the empirical coefficient needed for this has been adjusted to match the test data. Without this correction the apparent peak efficiency would not drop sharply as the speed decreases as shown in figure 13. The curves also include an extrapolation to a higher rotational speed, which was not measured, to demonstrate that the system still produces sensible characteristics at higher speeds.

A further case is shown in figure 14. This stage was not included in the stages used to generate the coefficients in the correlation equations, and is extremely well-predicted with the equations and coefficients derived from the other stages. Of great interest is the fact that this stage has a very high back-sweep leading to a work coefficient at the design point of only 0.5, compared to a value of 0.6 to 0.75 for the other stages. The consequence of this is that the steeper flow coefficient versus work coefficient relationship from equation 9 leads to steeper pressure rise characteristics. This effect cannot be predicted simply by scaling characteristics of other stages and demonstrates the predictive nature of the method adopted here.

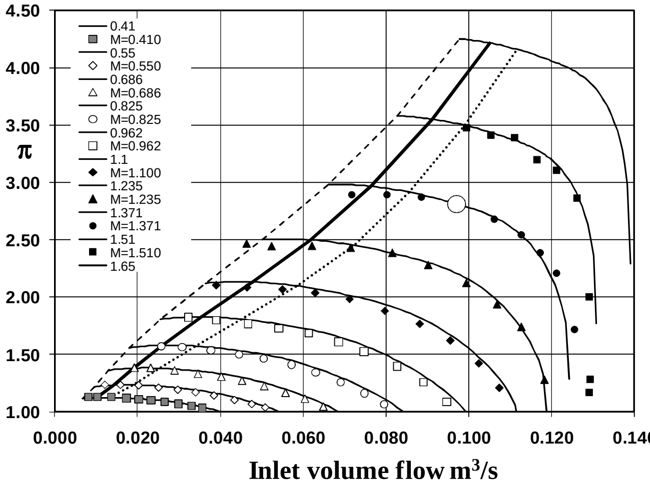

Figure 12: Predicted and measured pressure ratio performance map for a turbocharger with a vaneless diffuser over a wide range of rotational speeds. The coefficients used are derived from an analysis of many stages, including this one.

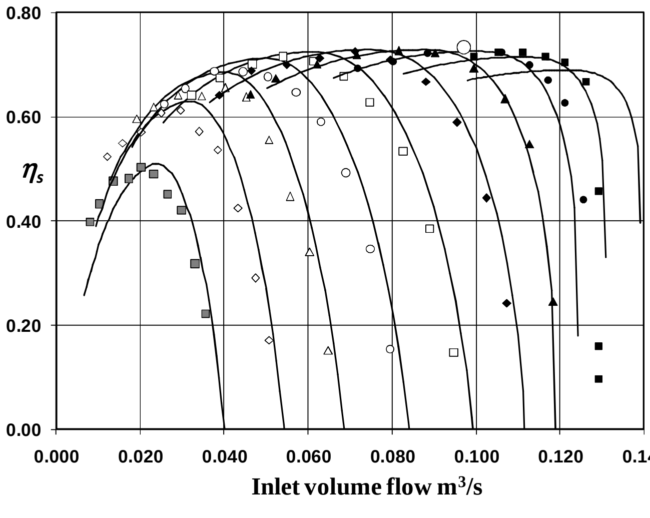

Figure 13: Predicted and measured efficiency performance map for a turbocharger with a vaneless diffuser over a wide range of rotational speeds. The coefficients used are derived from an analysis of many stages, including this one, and a correction for the effect of heat transfer at low speeds is made. Symbols as in figure 12.

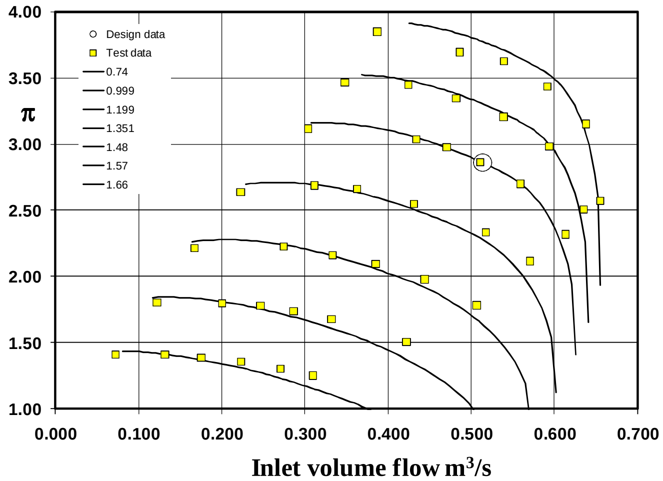

Figure 14: Predicted and measured pressure ratio performance map for a turbocharger with high back-sweep over a wide range of rotational speeds. This stage was not used to derive the correlations used here.

DISCUSSION AND OUTLOOK

The work presented here allows an estimate of the performance map of a centrifugal compressor stage to be obtained from limited design data during the preliminary design phase, without prior knowledge of the stage geometry. Most of the examples presented are for turbocharger compressor stages with vaneless diffusers, but in work not described in detail here the method has also been adapted to predict other categories of compressor stages by the use of different empirical coefficients in the equations.

The equations provide a fully parameterized system of algebraic functions for the shape of the performance map, which can also be used in different modes, in which the coefficients are adjusted to exactly match the measured performance of a particular stage. This then provides an algebraic set of equations for a performance map that could be used in whole engine performance calculations, allowing the performance for any flow and speed to be calculated extremely rapidly with very little data required and no detailed knowledge of the geometry. Alternatively a single measured speed line can be approximated and other speed-lines then generated by the equations.

The method has been developed on the basis of the inherent non-dimensional performance coefficients of the stages, and because of this can be adapted to other gases and other applications relatively easily. It has already been adapted to generate a stage stacking tool for multi-stage process compressors allowing the behavior of several stages of a multistage compressor to be analyzed.

An obvious limitation of the method is that it only considers the global performance data and not the component losses (impeller, diffuser and volute) which are the cause of this behavior. The method can naturally be developed further to include the individual components so that separate sets of performance curves for each component can be developed and stacked to produce a more accurate stage performance, which is actually the procedure suggested by Rodgers (1964) and used by Swain (1990). The extension to include the separate diffuser and impeller characteristics would also allow the method to identify in more detail the choking and instability limits of each component and to study changes in component matching with speed, and is currently being pursued.

The fact that such a simple technique can predict the shape of characteristics of compressor stages is of great relevance to the use of performance correlations. There are many competing correlation systems in the literature, see for example the extensive but non-exhaustive list provided by Oh et al (1997). All of these seem to do equally good jobs of predicting performance maps when the empirical coefficients have been tweaked appropriately. The important finding from this paper is that, provided the methods predict the peak efficiency point reasonably well, the variation away from this point is then fairly similar for all well-designed stages of a similar type and duty and can be predicted without the need for correlations of individual effects or information about the geometry.

CONCLUSIONS

The theoretical analysis and correlations in this paper provide a completely novel way of predicting centrifugal compressor performance maps during the preliminary design phase. The basis of the method is the scientific analysis of measured stage characteristics using classical non-dimensional parameters and the approximation of these with suitably designed parametric equations. The non-dimensional parameters predict a reasonably accurate performance map for a particular duty, based on experience from other stages, which can be used as a reference to quickly assess the operating range of a compressor against objectives for a new design. This method also produces an important new insight into the off-design performance – that for a well-designed stage this is also defined by the design duty. The weakest aspect of the method is the considerable uncertainty that remains with the prediction of the surge line, but an optimistic, a realistic and a pessimistic estimate can be made. It is hoped that the same equations when adapted to predict component performance will be more successful in respect of surge prediction.

The novel features of the method are:

- A new set of parameterized algebraic equations has been developed that describes the variation of efficiency with changes in flow and speed away from the design point.
- The method requires the values of only four key non-dimensional parameters at the design point (the efficiency, flow coefficient, work coefficient and tip-speed Mach number) to define the whole performance map and requires very little knowledge of the geometry.
- The equations are designed to automatically produce physically realistic behaviour of the characteristic curves

and include empirical coefficients that adjust the shape of the efficiency characteristics to match experimental data on different speed-lines of compressor stages.

- The variation of work input with changes in flow and speed away from the design point is determined from the Euler equation, using empirical data for the disc friction, the degree of reaction and the slip factor, also with no detailed knowledge of the geometry.
- The coefficients in all these equations have been calibrated from extensive test data on a range of compressor stages. Typical values of the necessary coefficients for well-designed turbocharger stages with vaneless diffusers are given in the paper.
- A new and useful form of presentation of the operating envelope of a compressor stage called, a “Flow coefficient-Mach” or a ϕ–Mach diagram, has been developed. This diagram is different for different stage types and highlights interesting aspects of the stage behavior related to mismatch at off-design speeds of stages with vaned and vaneless diffusers.
- The method has been described mainly for turbocharger compressor stages with vaneless diffusers but with different values of the empirical coefficients it is possible to adapt the same equations for use with stages with vaned diffusers and with industrial process impellers.

ACKNOWLEDGMENTS

The first author would like to thank the Rector of the University of Stuttgart for his permission to take a sabbatical term in 2009, which was material to the development of the method described here. The authors are indebted to the session organiser, Greg Holbrook, and the reviewers of the paper whose constructive comments on the first draft allowed many improvements to be made. Many companies involved in confidential development projects with PCA Engineers and with the University of Stuttgart are acknowledged for the provision of confidential measured compressor performance data used to carry out this analysis. The assistance of Ed Swain, Peter Came and Jeremy Tapper is gratefully acknowledged.

REFERENCES

[1] Aungier, R. H., (2000), *Centrifugal compressors – a strategy for aerodynamic design and analysis*, ASME Press, New York, USA.

[2] Cumpsty, N. A., (1989), *Compressor Aerodynamics*, Longman Group, Pearson Education Ltd, Harlow, Essex, U.K.

[3] Rodgers, C. (1964), “Typical performance characteristics of gas turbine radial compressors”, Trans ASME, Journal of Engineering for Power, Vol. 86.

[4] Swain, E., (1990), “A simple method for predicting centrifugal compressor performance characteristics”, Proceedings of IMechE Conference, C405/040, 1990.

[5] Swain, E., (2005), “Improving a one-dimensional centrifugal compressor performance prediction method”, Proc. IMechE Vol. 219 Part A: J. Power and Energy.

[6] Casey, M.V., (1994), "Computational Methods for Preliminary Design and Geometry Definition in Turbomachinery", AGARD-LS-195, AGARD Lecture Series on Turbomachinery Design using CFD, NASA-Lewis, 1994.

[6] Lohmberg, A., Casey, M., and Ammann S., (2003), “Transonic Radial Compressor Inlet Design”, Proc. IMechE, Vol. 217 Part A: J. Power and Energy.

[7] Casey, M. V. and Schlegel, M. (2010), “Estimation of the performance of turbocharger compressors at extremely low pressure ratios”, Proc. IMechE, Vol. 224 Part A: J. Power and Energy, pp 239-250.

[8] Gülich, J. F., (2008), *Centrifugal Pumps*, Springer, Berlin, Germany.

[9] Daily, J.W. and Nece, R.E., (1960), “Chamber dimension effects on induced flow and frictional resistance of enclosed rotating disks”, ASME Trans., J. Basic Engineering, Vol. 82, pp. 217-232.

[10] Casey, M. V. and Fesich, T. M. (2010), “The efficiency of turbocharger compressors with diabatic flows”, Trans. ASME, Journal of Engineering for Gas Turbines and Power, July 2010, Vol. 132 / 072302-1.

[11] Baines, N. C., (2005), *Fundamentals of Turbocharging*, Concepts/NREC, Vermont, USA, ISBN 0-933283-14-8.

[12] Oh, H.W., Yoon, E.S., Chung, M.K. (1997), “An optimum set of loss models for performance prediction of centrifugal compressors”, Proc. IMechE, Vol. 211 Part A: Journal of Power and Energy.

